Published in "The Journal of Physical Chemistry A 122(4): 1146–1155, 2018"
which should be cited to refer to this work.

Shape and Core-Excited Resonances in Thiophene

Published as part of The Journal of Physical Chemistry virtual special issue "Manuel Yáñez and Otilia Mó Festschrift".

Alexandra Loupas,[†,‡] Khrystyna Regeta,[¶,§] Michael Allan,[¶] and Jimena D. Gorfinkiel*[,‡]

[†]Laboratório de Colisões Atómicas e Moleculares, CEFITEC, Departamento de Física, Faculdade de Ciências e Tecnologia, Universidade Nova de Lisboa, Campus de Caparica, Lisboa, 2829-516 Portugal

[‡]School of Physical Sciences, The Open University, Walton Hall, Milton Keynes MK7 6AA, United Kingdom

[¶]Department of Chemistry, University of Fribourg, Fribourg 1700, Switzerland

Supporting Information

ABSTRACT: We present a comprehensive study of resonance formation in electron collisions with thiophene. Detailed calculations have been performed using the ab initio R-matrix method. Absolute differential cross sections for electron impact excitation up to 18 eV and for two scattering angles, 90 and 135°, have been measured. Agreement between the calculated and measured experimental cross sections is very good. Three shape resonances previously described, two of π^* character and one σ^*, as well as a number of resonances of core-excited or mixed character are identified and characterized in the calculations. The measured cross sections provide experimental confirmation for a number of the core-excited resonances. The link between these resonances and prior DEA experiments is discussed.

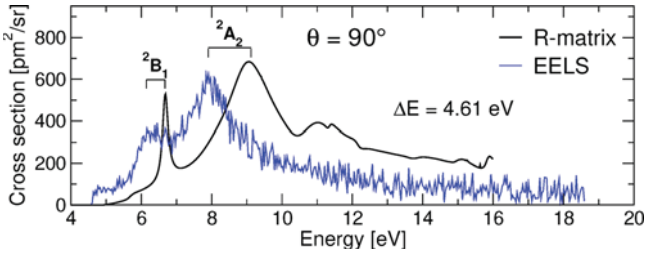

INTRODUCTION

The impact of low-energy electrons is well-known to cause bond cleavages in DNA.[1] This breakup is initiated through the formation of a negative ion transient state, commonly known as a resonance. Depending on its characteristics, this anionic state will either decay via autodetachment or lead to dissociation and the formation of two or more fragments, one of them negatively charged, during a process known as dissociative electron attachment (DEA).[2] Free and presolvated electrons are formed in large quantities when radiation interacts with biological matter.[3] Therefore, understanding DEA and resonance formation is crucial to the interpretation of how low-energy electrons induce DNA damage: a lot of work has been performed, both theoretical and experimental, especially on DNA constituents (in particular nucleobases), some amino acids, radiosensitizers and model molecules.[4,5]

This work presents the study of low-energy electron collisions with thiophene (C_4H_4S), one of the most used building blocks in anti-inflammatory drugs.[6] Thiophene is a prototypical, fully conjugated, heterocyclic molecule that contains one heavy and highly polarizable sulfur atom. Thiophene is also the main unit of several types of materials, such as polythiophene. When properly doped, polythiophene is conductive and has found application in electrochromic displays, electro-optic devices, protection against photocorrosion, and energy storage.[7] In other materials, thiophene's presence confers various important properties, making them promising as photochromatic molecular switches,[8] organic semiconductors,[9] solar cells,[10] light-emitting diodes, and field-effect transistors.[11] As all of these applications involve electron transfer, understanding thiophene's electronic structure and electron-induced processes is of great relevance.

Electron collisions with thiophene have been previously studied at both theoretical and experimental levels. The only DEA study was performed by Muftakhov et al.,[12] who recorded mass spectra in the gas phase in the energy range of 0−12 eV. They interpreted the peaks in these spectra as corresponding to seven resonant states mainly of Feshbach character, a couple of which lie above the ionization threshold and therefore are expected to correspond to core-excited resonances in which the electron is excited from a deeply bound orbital.

Asmis[13] measured electron energy loss spectra (EELS) for vibrational excitation and found three resonances at 1.27, 2.83, and 5.5 eV. He assigned the first two resonances as one-particle (i.e., shape) π^* resonances and the last one as a σ^* resonance. (A summary of the EELS can be found here: http://homeweb.unifr.ch/allanm/pub/ma/dir_allan/thiophene_EELS.PDF.)

Modelli and Burrow[14] obtained electron transmission spectra (ETS) for thiophene below ≃4.5 eV. They found two intense resonances at 1.15 and 2.63 eV, associated with electron capture into the two lowest empty π^* molecular orbitals, of b_1 and a_2 symmetry. They stated that the signal corresponding to an expected σ^* resonance (scaled virtual orbital energies in their

work put the σ^* resonance at around 2−2.1 eV) is probably masked by overlap with the high-energy tail of the lower, more intense π^* resonance.

Hedhili et al.[7] investigated electron stimulated desorption (ESD) of anions from multilayer thiophene condensed on a polycrystalline platinum substrate. The yield functions that they obtained show that anions are desorbed both by dissociative electron attachment, with peaks observed at 9.5, 11, and 16 eV, and for higher energies, via dipolar dissociation.

From the theoretical point of view, two methods have been been applied to the study of electron scattering from thiophene at low energies. First, da Costa et al.[15] reported electron impact integral elastic, momentum transfer, and differential cross sections calculated with the Schwinger multichannel method with pseudopotentials (SMCPP) for energies ranging from 0.5 to 6 eV. They identified two π^* and a σ^* shape resonances, the latter with a strong d-wave character. Vinodkumar et al.[16] used the R-matrix method (through the QUANTEMOL-N interface) for low-energy calculations and the Spherical Complex Optical Potential formalism for intermediate to high energy. Their R-matrix calculations are similar to those presented in this paper; however, their results (see later) are very different and show a number of inconsistencies. No work has focused on core-excited resonances. Finally, we note that Mozejko et al.[17] calculated integral elastic and ionization cross sections at intermediate and high electron impact energies using the additivity rule approximation and the binary-encounter Bethe approach.

In this work, we have investigated resonance formation in thiophene both experimentally and computationally. We have used the R-matrix method,[18] as implemented in the UKRmol suite,[19] to investigate electron collisions with thiophene in its equilibrium geometry. We have performed the calculations at different levels of complexity to identify and characterize both shape and core-excited resonances. We have also determined the excitation function (i.e., angular differential cross sections as a function of incident electron energy for a specific energy loss) by means of EELS. Both the calculated data and the detailed excitation functions show the presence of a number of mixed and core-excited resonances, some of which can be correlated with peaks in DEA anion yields.[12]

THEORY

R-Matrix Method. We performed our scattering calculations within the fixed-nuclei approximation, that is, keeping the nuclei fixed at the ground state equilibrium geometry of the molecule. The R-matrix method has been described in detail elsewhere;[18,20] therefore, we present only a brief description here.

The basic idea of this method is the division of the configuration space into two regions, separated by a sphere of radius a, the R-matrix sphere. In the inner region, correlation and exchange effects between all electrons play a crucial role and have to be considered. In the outer region, exchange between the scattering electron and the electrons of the target system can be neglected. It is crucial for the applicability of the method that the radius of the R-matrix sphere be chosen in a way that it contains the charge densities of the relevant target electronic states and the $N + 1$ electron functions χ_i defined below.

In the inner region, we describe the system using a set of basis functions Ψ_k of the form

$$\Psi_k = \mathcal{A} \sum_{i=1}^{n} \sum_{j=1}^{n_c} \Phi_i(\mathbf{x}_N;\, \hat{r}_{N+1};\, \sigma_{N+1}) \frac{u_{ij}(r_{N+1})}{r_{N+1}} a_{ijk} + \sum_{i=1}^{m} \chi_i(\mathbf{x}_{N+1}) b_{ik} \quad (1)$$

where $\mathcal{A}$ is the antysimmetrization operator; Φ_i are the wave functions describing the target electronic states, and $\mathbf{x}_N$ and $\mathbf{x}_{N+1}$ represent spin and space coordinates of all N and $N + 1$ electrons, respectively. σ_{N+1} stands for the spin of the $(N + 1)$th scattering electron, and r_{N+1} and $\hat{r}_{N+1}$ represent its radial and angular coordinates, respectively. The functions $\frac{u_{ij}(r_{N+1})}{r_{N+1}}$ describe the radial part of the wave function of the scattering electron, while the L^2 integrable functions χ_i are necessary for a good description of the short-range polarization-correlation effects. Finally, the coefficients a_{ijk} and b_{ik} are determined by the requirement that the functions Ψ_k diagonalize, in the inner region, the electronic nonrelativistic Hermitian Hamiltonian of the $(N + 1)$-electron system.[20]

In the outer region, the wave function describing the scattering electron is approximated by a single-center, partial wave expansion, reducing drastically the computational cost. Having obtained the basis functions Ψ_k, the R-matrix is built and propagated to the asymptotic region, where the K-matrix is obtained. From the K-matrix, one can determine the S-matrix and, from it, the cross sections. Both K- and S-matrices can be used to identify and characterize resonances.

In our study, we included partial waves up to $l = 4$ (and tested, for the smaller calculations, $l = 5$). Inclusion of higher partial waves increases the computational cost of the calculations significantly. Additionally, this partial wave expansion does not converge in the fixed-nuclei approximation for polar molecules. This lack of convergence is usually circumvented by means of a Born correction.[21] However, given the relatively small dipole moment of thiophene (see below), we have not included this correction: it only affects dipole-allowed transitions, and the effect for electronic excitation in the energy range of interest has been shown to be small (around 5%) even for molecules with a much larger dipole moment (for example, pyridine[22] with $\mu = 2.33$ D). The effect of not including the correction will be to underestimate the elastic and total cross sections, most visibly at low energies, and the cross sections for excitation into singlet states at higher energies.

Angular differential cross sections for electronic excitation are calculated following a well-established methodology based on the adiabatic nuclei approximation[23,24] using a program developed by Z. Mašín. The approach uses the T-matrix (trivially obtained from the S-matrix) calculated with the R-matrix method.

Different levels of approximation can be employed in scattering calculations, and these are determined by the choice of target electronic states (how many) and the type of the L^2 functions included in the eq 1. The Static-Exchange (SE) and Static-Exchange plus Polarization (SEP) approximations use a Hartree−Fock description of the ground electronic state of the target, the only state included in the calculation. These approximations are capable of describing resonances in which the target molecule remains in the ground state, known as shape resonances. In the SEP approximation, the molecule is allowed to be polarized by the incoming electron. This effect is modeled by including the appropriate L^2 configurations

$$\chi_i:\ (\text{core})^{N_c}(\text{valence})^{N-N_c}(\text{virtual})^1 \quad (2)$$

$$\chi_i:\ (\text{core})^{N_c}(\text{valence})^{N-N_c-1}(\text{virtual})^2 \quad (3)$$

where the core orbitals are always doubly occupied by N_c electrons. The valence space is defined here as those orbitals occupied in the ground state configuration that are not core orbitals.

Single excitations from the valence to a selected number of virtual orbitals (VOs), which are also available for the incoming electron, are allowed. Due to the presence of these single excitations from the valence space to a VO, the SEP model can sometimes describe (poorly) core-excited resonances.

The Close-Coupling (CC) method is necessary for the accurate description of core-excited resonances, i.e., resonances in which the electron excites the molecule as it attaches itself to it. In this case, wave functions corresponding to a number of excited states of the target are included in eq 1. These are usually described at the Complete Active Space (CAS) level. Here, the L^2 configurations take the following form

$$\chi_i: (\text{core})^{N_d}(\text{CAS})^{N-N_d+1} \tag{4}$$

$$\chi_i: (\text{core})^{N_d}(\text{CAS})^{N-N_d}(\text{virtual})^{1} \tag{5}$$

where the active space (CAS) includes both occupied and unoccupied orbitals of the ground state configuration. Therefore, the virtual space is different from that of the SEP L^2 configurations; similarly, more orbitals are normally treated as core orbitals here to keep the size of the calculation feasible.

Whereas the choice of active space is guided by conventional computational chemistry considerations and the number of excited states to be included at the CC level is determined by the range of scattering energies to be studied, choosing how many VOs to include in the above configurations is not straightforward: not enough VOs will lead to a poor description of polarization effects. Too many VOs can lead to overcorrelation of the $N+1$ wave functions; in this case, resonances will appear lower in energy than they physically are. As we will see later, the choice of VOs has not been straightforward in this work.

Time Delay Analysis. The main focus of this work is resonance identification and characterization. One common way to find resonances is to look at the cross sections, although this approach is not always reliable; peaks corresponding to physical resonances may be masked by other resonances or the non resonant contribution to the scattering processes, and features that look like peaks may not actually correspond to resonances. Another quantity that allows resonance identification is the eigenphase sum, obtained from diagonalizing the K-matrix. It was shown by Hazi[25] that an isolated resonance manifests itself as a characteristic jump of approximately π in the eigenphase sum in the energy region centered around the position of the resonance. However, resonances may also be difficult to identify in the eigenphase sum when they overlap or the nonresonant contribution is significant.[26]

Analysis of the time delay enables the unambiguous identification of resonances even in cases in which the eigenphase sum does not show the typical resonant behavior. A description of the method and its applications as well as its advantages over the conventional eigenphase sum analysis have been reviewed in detail before.[27]

We use the definition of the time delay as formulated by Smith:[28] the **Q**-matrix, the time delay matrix, at a given energy is calculated directly from the **S**-matrix

$$\mathbf{Q}(E) = i\hbar\mathbf{S}\frac{d\mathbf{S}}{dE} \tag{6}$$

The process of searching for resonances involves analysis of the positive eigenvalues (time delays) and associated eigenvectors of the **Q**-matrix for each energy. Resonances appear as a Lorentzian peak in these eigenvalues. Those time delays much larger than $\hbar/E$ can be interpreted as arising from resonant processes and can be fitted using

$$\frac{\hbar\Gamma_\alpha}{(E-E_\alpha)^2+(\Gamma_\alpha/2)^2} + 2\hbar\frac{d\delta_{bg}}{dE} \tag{7}$$

where E_α and Γ_α are, respectively, the position and width of resonance α and δ_{bg} is the background contribution to the eigenphase sum, weakly dependent on energy.

The analysis of the time delay also allows us to characterize the resonances in terms of their parent state(s). The square of the jth coefficient of the eigenvectors of $\mathbf{Q}(E)$ corresponding to a resonance ($|c_j|^2$) is equal to the branching ratio, which gives the probability of decay of a metastable state into the jth channel and, consequently, can be used to determine the parent states of shape and core-excited shape resonances.

In this work, we used the inspection of the time delay to identify and characterize all resonances.

EXPERIMENTAL APPROACH

EELS and measurements of energy dependence spectra (also called excitation functions) were performed using a well-tested spectrometer with hemispherical analyzers[29,30] and employing procedures used previously to study electron scattering from targets like furan[31] and pyrimidine.[32,33] The spectrometer uses hemispherical analyzers to improve resolution. The electron beam current was 300−700 pA. The energy of the incident electrons was calibrated on the 19.365 eV ^2S resonance in helium[34] and is accurate to within ±10 meV. The sensitivity of the instrument depends on the electron energies. This effect, expressed as the "instrumental response function", was quantified on elastic scattering in He; all of our spectra were corrected as previously described.[29,30] The technicalities of "tuning" the instrument and of determining the response functions have been described in previous work,[29,30] particularly on N_2.[35]

The absolute values of the excitation functions were determined by comparing the areas under the elastic peak and under the electronic excitation bands of interest, as previously described.[31] The required absolute values of the elastic cross sections (presented in the Supporting Information) were determined by the relative flow technique as described by Nickel et al.[36] using, as a reference, the theoretical helium elastic cross sections of Nesbet.[37] The confidence limit is ±15% for the elastic cross sections and ±25% for the inelastic cross sections and excitation functions.

COMPUTATIONAL DETAILS

Thiophene, C_4H_4S, is a planar molecule that belongs to the C_{2v} point group. It contains 44 electrons and has a dipole moment of 0.52 D.[38] Its experimentally determined polarizability[39] is 60.8 a_0^3, and its ionization energy is 8.86 eV.[40] Thiophene is an asymmetric top, and its first electronic excitation threshold is around 3.7 eV.[13,41−43]

In our calculations, we have used the molecular geometry listed on the NIST Web site, calculated at the MP2 level using the cc-pVDZ basis set.[40]

Target Model. The electronic excited states of thiophene have been studied by a number of experimental and theoretical groups. Flicker et al.[43] performed electron impact experiments at scattering angles from 0 to 80° and impact energies of 30 and 50 eV to study the lowest singlet−triplet transitions of thiophene. Palmer et al.[41] investigated the VUV and EELS spectra of thiophene and assigned the bands by means of high-level multireference multiroot CI studies, with several basis sets. Haberkern et al.[42]

Table 1. Calculated Vertical Excitation Thresholds (in eV) of the Electronic States Included in the CC Calculation[a]

	ours	ref 44	ref 49	ref 46	ref 47	CASSCF	PT2F	exp.
$1\ ^3B_2$	3.722	3.53	3.39	–	3.94	3.83	3.75	3.7,[53] 3.72[13b] 3.75,[43] 3.74[41,42]
$1\ ^3A_1$	4.943	4.35	4.33	–	4.86	4.90	4.50	4.6,[53] 4.61[b] 4.62[13,41−43]
$1\ ^1A_1$	5.916	5.39	5.24	5.64	5.41	6.41	5.33	5.41[b], 5.43[13,41,42] 5.45,[13] 5.48[43]
$1\ ^3B_1$	6.371	5.65_R	5.69	–	5.94_R	5.93	5.90	5.9[b]
$1\ ^3A_2$	6.457	5.77_R	5.64	–	5.75_R	5.57	5.88	5.9[b]
$1\ ^1B_1$	6.660	5.86_R	5.88	6.17	5.87_R	6.72	6.23	–
					⋮			
$2\ ^3A_1$	6.816	–	5.63	–	–	–	–	–
$1\ ^1A_2$	6.877	5.88	5.72	6.23	6.41_R	6.43	5.93	5.9,[43] 6.0[52,54]
$2\ ^3B_2$	6.906	–	5.99	–	–	–	–	–
$1\ ^1B_2$	6.952	5.54	5.42	5.97	5.72	8.10	5.72	5.52,[41] 5.61[13,42] 5.65,[55] 5.77[51]
					⋮			
$2\ ^1A_1$	8.060	–	7.03	7.38	6.73	8.85	6.69	6.6,[53] 6.7[52]
					⋮			
$2\ ^1B_2$	9.411	–	–	6.97	6.41_R	6.79	6.56	7.1[43]
$3\ ^3A_1$	9.563	–	–	–	–	–	–	–
$2\ ^3A_2$	9.731	5.80_R	–	–	–	–	–	–
$2\ ^1A_2$	10.055	6.10_R	6.33	–	6.73_R	7.50	6.97	–
$3\ ^3B_2$	10.116	–	–	–	–	–	–	–
$4\ ^3B_2$	10.139	–	–	–	–	–	–	–
$5\ ^3B_2$	10.368	–	–	–	–	–	–	–
$3\ ^1B_2$	10.630	–	–	7.69	7.12_R	7.44	7.28	–
$3\ ^1A_1$	10.749	–	–	7.65	7.32	7.46	7.23	–
$2\ ^3B_1$	10.827	–	6.18	–	–	–	–	–
$3\ ^3A_2$	11.046	–	6.11	–	–	–	–	–
$6\ ^3B_2$	11.247	–	–	–	–	–	–	–
$4\ ^3A_1$	11.422	–	–	–	–	–	–	–

[a]Previous results are from calculations, Salzmann et al.,[44] Kleinschmidt et al.,[49] Holland et al.,[46] Nakatsuji et al.,[47] and Merchán et al.[48] (both CASSCF and PT2 results are presented); experiments, Moodie et al.,[51] Zauli et al.,[52] Flicker et al.,[43] van Veen et al.,[53] Asmis,[13] Haberkern et al.,[42] and Veszpremi et al..[54] The energies labeled with an *R* correspond to Rydberg states. The vertical dots (⋮) indicate that several other states are present in that calculation in this energy range. [b]The energies of the states identified in our EELS spectra.

measured high-resolution EELS spectra in the range of the low-lying singlet−triplet excitations. In combination with ab initio calculations, the spectral structures were assigned and adiabatic transition energies were determined. Salzmann et al.[44] used time-dependent Kohn−Sham density functional theory combined with a density functional/multireference configuration interaction method (DFT/MRCI) to explore the ground and low-lying electronically excited states of thiophene in order to explain the ultrafast decay of low-lying vibrational levels of the lowest singlet state, observed by time-resolved pump−probe femtosecond multiphoton ionization spectroscopy.[45] Holland et al.[46] used synchrotron radiation-based Fourier transform spectroscopy to study the excited states of thiophene. A highly resolved photoabsorption spectrum was measured between 5 and 12.5 eV, combined with high-level ab initio calculations that used the second-order algebraic-diagrammatic construction polarization propagation approach and the equation-of-motion coupled-cluster (EOM-CC) method at the CCSD and CC3 levels to assign the spectrum. Nakatsuji et al.[47] used the symmetry-adapted cluster configuration interaction (SAC-CI) method and a basis set augmented with diffuse Rydberg functions to describe a large number of Rydberg states. Merchán et al.[48] studied the electronic spectrum of thiophene using multiconfiguration second-order perturbation theory and the extended ANO basis set. Their results were used to assign the experimental spectrum below 8 eV. Kleinschmidt et al.[49] used SPOCK (a code that calculates spin−orbit matrix elements in the one-center mean-field approximation for multireference CI wave functions) and the DFT/MRCI approach to provided excitation energies in good agreement with the experiments.

For our calculations, we tested two different basis sets: cc-pVDZ and 6-311G**. Because, as prior work identified, thiophene possesses a significant number of low-lying Rydberg states, the 6-311G** basis set produced results closer to those of experiments. Therefore, throughout this work, we present results obtained with this basis set. We note, however, that our calculations do not describe the Rydberg states well.

Hartree−Fock SCF (HF) and state-averaged CASSCF orbitals were generated using MOLPRO[50] and used in the scattering calculations. In the state-averaged CASSCF calculations, we used the active space of (10,9) (10 electrons distributed among 9 orbitals) and included in our state-averaging seven states: $1-2^1A_1$, $1-3^1B_1$, 1^1B_2, 1^1A_2. The ground state configuration of thiophene is $1a_1^2 2a_1^2 1b_2^2 3a_1^2 2b_2^2 4a_1^2 3b_2^2 5a_1^2 1b_1^2 6a_1^2 7a_1^2 4b_2^2 8a_1^2 5b_2^2 9a_1^2 6b_2^2 10a_1^2 7b_2^2 2b_1^2$-$11a_1^2 3b_1^2 1a_2^2$. The active space comprised the orbitals $11-12a_1$, $7-8b_1$, $2-4b_2$, and $1-2a_2$. The ground state energies and dipole moments obtained are, for the HF and CASSCF calculations, −551.343 and −551.428 hartree and 0.722 and 0.549 D.

Table 2. Positions and Widths (in brackets) in eV of the Low-Lying Shape Resonances in Thiophene Taken from Our Time Delay Analysis[a]

	present results				other calc.		exp.	
resonances	SEP		CC	VAE	ref 15	ref 16	ref 13	ref 14
	35 VO	41 VO						
π_1^* (B_1)	0.949	0.80	1.114	0.95	1.00	2.51	1.27	1.15
	(0.035)	(0.020)	(0.05)	–	(0.33)			
σ^* (B_2)	2.990	2.51	~1.5	2.11	2.78	18.69	–	–
	(2.35)	(2.107)	(2.26)	–	(1.10)	–	–	
π_2^* (A_2)	2.993	2.87	2.909	3.10	2.82	4.35	2.83	2.63
	(0.438)	(0.340)	(0.48)	–	(1.28)			

[a]The SEP results were calculated for 35 and 41 VOs. VAEs are also presented. We list the calculated results from da Costa et al.[15] and Vinodkumar et al.[16] and the experimental positions obtained by Asmis[13] and Modelli and Burrow.[14].

Table 1 lists the vertical excitation energies of the 25 states (ground state + 24 excited states) included in the CC calculation together with the most relevant prior theoretical and experimental results. We observe that the agreement between our results and both theory and experiment gets worse as the energy increases. This agreement is reasonably good for the first few states, but differences of several eV occur for the higher states. We note that the calculations of Nakatsuji et al.[47] produce a large number of Rydberg states not described by ours; the more diffuse basis sets that would be needed to describe these states (and improve the description of other Rydberg states) would entail the use of much bigger radii. Unfortunately, with the UKRmol suite, this would lead to either serious linear dependence problems or a significant decrease in the quality of the continuum description.[18] This poor and incomplete description of the Rydberg states in our calculations means that any resonances associated with them will either not be described or described poorly.

Scattering Model. A radius of $15a_0$ was required for the R-matrix sphere for the calculation as the 6-311G** basis set was used. We included partial waves up to $l = 4$; the effect of adding $l = 5$ was tested at the SEP level, and no significant changes were observed in the resonance positions. In the UKRmol suite, the continuum orbitals are Schmidt orthogonalized to the orbitals of the target; the resulting continuum orbitals face a symmetric orthogonalization, where the deletion threshold was set to 1×10^{-7}.

We performed the calculations at SE, SEP, and CC levels, freezing 9 and 17 core orbitals (i.e., $N_c = 18$ and $N_d = 34$ in eqs 3 and 4) in the latter calculations, respectively. For molecules with significant polarizability, a good description of the resonances (their position and width) depends strongly on the quality of the description of the polarization effects. As explained above, this depends on the number of VOs included in the calculation, but unfortunately, convergence is not possible. Our approach[26,56] is therefore to start with a small number of these orbitals and keep adding more, in order of increasing energy, until good agreement is found with the experimental positions of shape resonances. If no experimental results are available, the number of VOs "optimized" for a similar molecule is used (for example, for the case of pyridazine, the numbers used for pyrazine and pyrimidine were employed[26]). This approach tends to under-represent polarization in the CC calculations but provides sufficiently accurate results for an effective comparison with experiments. From this procedure, we determine that the optimal number of VOs to include in our SEP and CC calculations was 35 and 70, respectively.

RESULTS

Low-Energy Resonances. Our calculations reveal, as expected, the presence of two low-lying π^* resonances, which are characteristic of molecules in which two double bonds are present and that were already identified in earlier experimental and theoretical work.[13−16] They also reveal the presence of a σ^* resonance, previously identified in calculations.[15] Table 2 lists the positions and widths of these three low-lying resonances determined at SEP and CC levels and compares them with the data available in the literature.

The positions of the resonances calculated at the SEP level agree well with those of da Costa et al.[15] calculated at the same level. (Their geometry is slightly different from ours, but in SE tests, this leads to shifts smaller than 0.1 eV in the resonance positions.) The π^* resonances also agree reasonably with the vertical attachment energies (VAEs) determined from the application of the scaled Koopman's theorem using Hartree−Fock orbitals obtained with the 6-31G* basis set. The position of the σ^* resonance determined from the VAE is significantly lower than that obtained from SEP scattering calculations. The results of Vinodkumar et al.[16] overestimate all resonance positions, either because of a poor description of polarization effects or simply because of an incorrect assignation of the resonances.

The positions of the π^* resonances determined experimentally are in good agreement among themselves and with the theoretical results. For reasons explained below, we present SEP R-matrix results using two different numbers of VOs. The effect of increasing the number of VOs by 6 is negligible in the A_2 π^* resonance but lowers the B_1 π^* one by around 0.15 eV and the σ^* resonance by around 0.4 eV.

Prior experience of describing π^* shape resonances in molecules containing a carbon ring[26,56] indicates that these resonances are better described in SEP calculations where sufficient L^2 configurations can be included to describe polarization. Therefore, it is generally the case in our calculations that the positions of pure π^* shape resonances determined using the CC method are higher than those determined in SEP calculations. When this is not the case, the fact is used to identify the resonances as mixed core-excited shape because it is understood that it is the inclusion of excited states in the CC expansion that improves the description of the resonance and thus lowers its position.[26,56]

This behavior is clearly shown by the first π^* resonance (see Table 2); our best CC calculation puts it above our best SEP calculation. In the case of the second π^* resonance, SEP and CC calculations seem to give a similar position. However, the σ^* resonance appears at significantly lower energy in the CC calculation. This behavior could be interpreted as indicating that the σ^* resonance has mixed character. This is unlikely to be the case for two reasons: (i) the lowest excited state is at 3.7 eV in our calculation, more than 2 eV above this resonance; (ii) being below its excited parent state, the resonance could only decay to

the ground state. This tends to make resonances longer lived and therefore narrow. The σ^* resonance is more than 2 eV wide.

One could argue that this "unusual behavior" may simply be due to the wrong number of VOs being chosen in the calculations. However, the choices presented here lead to π^* resonances with positions in very good agreement with experiment. As Table 2 shows, increasing the number of VOs in the SEP calculation lowers the π^* resonances below their experimental positions. Inclusion of fewer VOs in the CC calculation leads either to fairly small changes (if 50 VOs are used, the upward shift in the position of all three resonances is on the order of 0.2 eV) or a shift that makes agreement for the π^* resonances much worse (when 30 VOs are used, the σ^* resonance is centered, in the time delay, at around 2.3 eV; however, the π^* resonances appear at approximately 1.5 and 3.3 eV).

We believe that our usual recipe (of including more VOs until reasonable agreement with experiment for all pure shape resonances is reached) cannot be applied here. This may be due to the fact that, unlike all earlier cases analyzed, this target has a mix of σ^* and π^* resonance or to a more subtle effect. Careful investigation of calculations at SE/SEP and CCs level indicated that inclusion of polarization effects has a bigger effect for the σ^* resonance at both levels. However, whereas when polarization is included in an SE calculation (when 35 VOs are used in the SEP model), the shift is of around 2.4 eV for the σ^* resonance and around 1.8−1.9 eV for the π^* one; in the CC case (comparing a calculation where no VOs are used to the one with 70 VOs; note that even when no VOs are used in the CC calculation, the inclusion of excited states and L^2 functions of the type in eq 4 already describes some amount of polarization), the shift for the σ^* resonance is around 2.5 eV, but for the π^* ones, it is 1.2−1.4 eV. It is possible, therefore, that our CC calculation with 70 VOs overestimates the polarization effect in the B_2 symmetry, placing the σ^* resonance too low in energy. As a result, we cannot conclude confidently where we would expect the σ^* resonance to appear in experiments; Modelli and Burrow's comment[14] would put it closer to the 1.5 eV of our CC calculations, but the calculations of da Costa et al. and VEAs would indicate a position above 2 eV. It is worth noticing that the maximum of the peak associated with the σ^* resonance in the total cross section calculated at the CC level appears at around 0.5 eV higher than that in the time delay. This can be seen in Figure 1 where the contributions to the cross section calculated at the SEP and CC levels are shown. This is not the case for the SEP calculations,

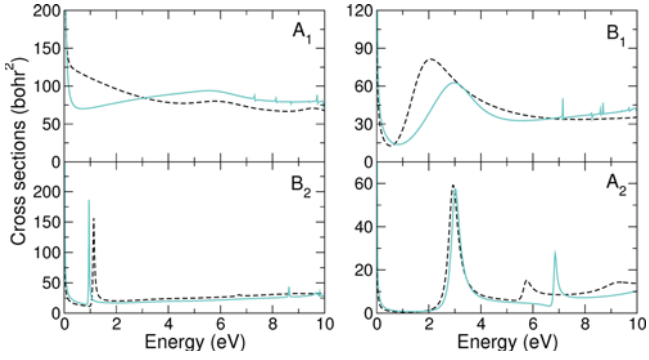

Figure 1. Contribution to the total cross section from the four irreducible representations of the C_{2v} point group. The dashed black line corresponds to the CC calculation, and the solid light blue line corresponds to the SEP calculation with 35 VOs. Note that no Born-type correction (see the text) has been added to these cross sections.

where the difference in position is around 0.1 eV. We believe that this indicates that the CC calculations are modeling a strong contribution of nonresonant scattering for the $^2B_2$ symmetry that shifts the resonance peak in the cross section.

Higher-Energy Resonances. The time delay obtained at SEP (35 VOs) and CC levels is presented in Figure 2. The figure

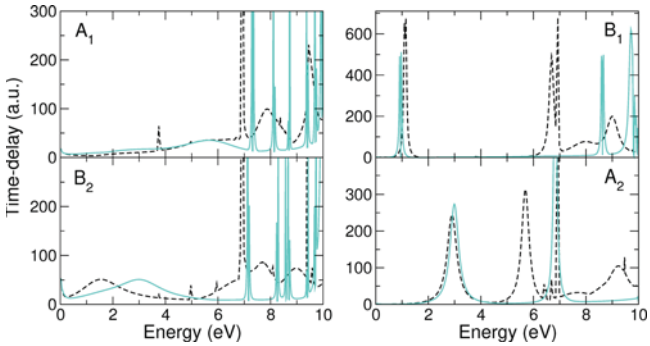

Figure 2. Largest eigenvalue of the time delay matrix for the scattering symmetries indicated in the panels. The dashed black line corresponds to the CC calculation, and the solid light blue line corresponds to the SEP calculation with 35 VOs.

is divided into four panels, each corresponding to one of the four irreducible representations of the C_{2v} point group. Above the first excitation threshold, the SEP calculations suffer from the presence of nonphysical pseudoresonances (that manifest as narrow peaks appearing above a certain energy), preventing us from providing reliable information on any physical resonances that may appear in that region. One should also notice that all of the CC time delays in Figure 2 have one prominent peak at 6.95 eV, corresponding to one of our excitation thresholds (thresholds are very often visible as narrow peaks/spikes in the time delay). A summary of the higher resonances found is presented in Table 3.

The first panel in Figure 2 presents the results for symmetry A_1. The very narrow peaks in the SEP results are probably pseudoresonances, whereas in the CC calculation we observe two broad peaks corresponding to physical resonances, at 7.9 and 9.5 eV. It is hard to tell whether there are corresponding peaks at the SEP level, but because no higher-energy resonances appear in our SE calculation, we believe that these are pure core-excited resonances. In addition, a wide structure is visible in the SEP time delay centered at around 5.7 eV. The feature is less obviously present in the CC time delay, but an analysis of the second largest eigenvalue of the **Q**-matrix does indicate a peak centered at around a similar energy. A resonance also appears in the SE calculations at ∼8 eV. Therefore, this feature could correspond to a shape resonance. Investigation of the orbitals that contribute to its description indicate that they have some contribution of CH bond character. The measured excitation function for the first triplet states (see the left-hand panel of Figure 3) displays a small band at 4.2 eV to which experimental considerations would assign B_1 symmetry and shape character, although no corresponding structure was found by Asmis. It is possible that this experimental peak corresponds to this resonance, despite the inconsistency in the symmetry.

The different positions of the σ^* resonance calculated at the SEP and CC levels (2.97 and around 1.5 eV, respectively), are clearly visible in the panel for the B_2 symmetry. Two other peaks appear in the CC time delay at around 7.7 and 9 eV. These correspond to core-excited resonances. In addition, there is a feature at ∼6.9 eV that is hidden in Figure 2 as it overlaps with the peak

Table 3. Positions and Widths in Brackets (in eV) of the Higher-Energy Resonances in Thiophene[a]

res.	E_R (width)	character	PS	EELS	ref 13
1^2A_2	5.695 (0.329)	MCES	1^3B_2, gs	5.4−5.5	5.38
1^2B_1	6.70 (0.172)	CE	$1^3A_1,1^3B_2$	6.4−6.45	6.22
1^2B_2	6.9 (1.85)	CE	–	–	–
2^2B_2	7.72 (1.15)	CE	1^3A_2	–	–
1^2A_1	7.87 (1.00)	CE	$1^1B_2,1^1B_1$	–	–
2^2B_1	7.96 (1.20)	MCES	$1^3B_2,1^3A_1$, gs	7.3−7.5	7.39
3^2B_2	8.98 (1.35)	CE	$1^1B_2,1^1A_1$	–	–
3^2B_1	9.01 (0.58)	MCES	$1^3B_2,1^1B_2$, gs	–	–
2^2A_2	9.22 (0.95)	CE	$1^3A_1,2^3A_1,1^3B_2$	8.0−8.1	7.93
2^2A_1	9.48 (0.2)	CE	$1^3A_2,1^1A_2$	–	–

[a]The position of the resonances in the EELS spectra are given as ranges determined from the positions of the peaks in the excitation functions for two angles (see Figure 3). We also list the experimental positions obtained by Asmis.[13] CE stands for pure core-excited resonances, MCES for mixed core-excited shape resonances, and gs for ground state. The most likely parent states (PS) have been obtained from the branching ratios when possible.

corresponding to the 7.7 eV resonance but corresponds to a resonance too. This hypothesis is confirmed by the analysis of the eigenphase sum. No resonances appear in the SE calculation above the σ^* shape resonance; therefore, all of the B_2 resonances are of core-excited character. None of them are visible in the total cross section shown in Figure 1.

The upper panel on the right corresponds to the B_1 symmetry. This is where the first π^* resonance appears, at 0.93 and 1.12 eV at the SEP and CC levels, respectively. At higher energies, three more resonances are observed in the time delay analysis: at 6.7 eV, near a threshold, there is a very well defined peak corresponding to a core-excited resonance; a broader feature appears at almost 8 eV with core-excited character; and finally, at 9 eV, it is possible to observe a well-defined peak. Interestingly, a peak is visible slightly above at SEP level; this peak is much wider than the ones we identify as pseudoresonances; therefore, we believe that this peak is likely to be physical. The analysis of the branching ratios indicates that all of these resonances have mixed shape core-excited character. Again, the resonances are not visible in the total cross section.

Finally, the A_2 symmetry presented in the last panel shows the second shape π^* resonance discussed earlier (see Table 2). A second resonance present at around 5.7 eV in the CC calculation has its corresponding peak at the SEP level appearing almost 1 eV higher. One other resonance, of core-excited character, is located at 9.2 eV. The structure (looking like truncated peaks) between 6 and 7 eV is hard to discern; it may just correspond to the thresholds or be linked to Feshbach resonances. Our calculations, however, do not identify any Feshbach resonances.

Table 3 summarizes the resonance positions and widths for the CC calculation, as well as the positions obtained from the experimental excitation functions (see below). The resonance positions

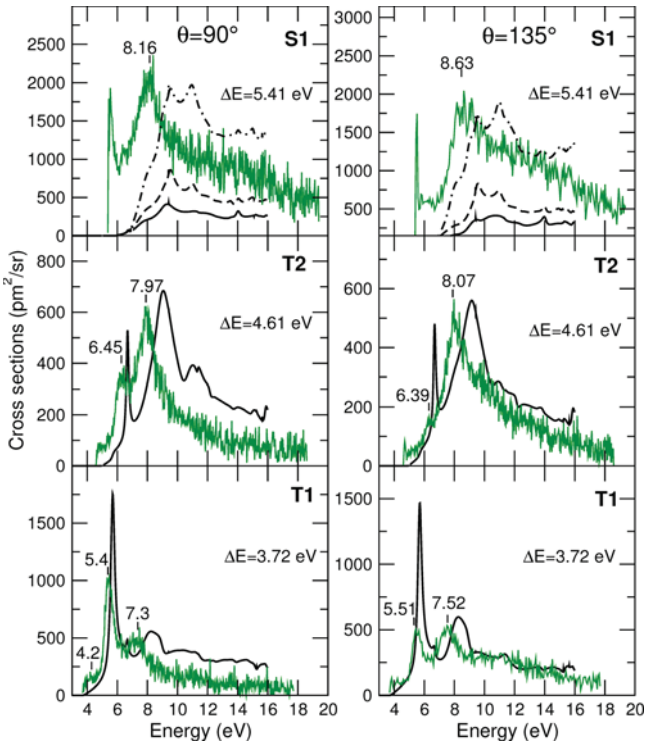

Figure 3. Calculated (black lines) and measured (green line) excitation functions for the energy losses indicated in the panels: left panels, scattering angle of 90°; right panels, scattering angle of 135°. The peaks of the measured excitation functions are also indicated in the panels. For ΔE = 5.41 eV, the full black line corresponds to excitation into the first excited singlet state only, whereas the dashed and dotted−dashed lines correspond to the sum of excitations into 3 and 7 states, respectively. See the text for more details.

are in good agreement with those of Asmis.[13] Although Vinodkumar et al. present data for a number of core-excited resonances, we have chosen not to include their results in the table as it is fairly clear that they are incorrect; all of their core-excited resonances appear well above (between 3 and 10 eV) the ionization threshold. This can be directly linked to the fact that, in their work, the excitation energies of the parent states are much higher than those in experiments. An inadequate description of polarization effects may also be contributing to the poor quality of Vinodkumar et al.'s results.

Excitation Functions. The experimental and theoretical excitation functions for two different electron scattering angles, 90 and 135°, are presented in Figure 3. Our energy loss spectra (see the Supporting Information) place the first triplet state (1^3B_2, T1) at 3.72 eV, the second (1^3A_1, T2) at 4.61 eV, and the first singlet state (1^1A_1, S1) at 5.41 eV. For this reason, the excitation functions were measured for energy losses, ΔE, of 3.72, 4.61, and 5.41 eV. However, the band centered at around ~5.6 eV in the energy loss for for 135° shows the likely presence of another triplet state (or states) that partly overlaps with the S1 state. Therefore, the excitation function labeled S1 actually corresponds to the excitation of several states of thiophene, though it is difficult to determine which and how many. We have therefore plotted three calculated curves for the ΔE = 5.41 eV energy loss: one (solid black line) corresponding to the excitation into the lowest singlet excited state (S1) only, another one (dashed line) corresponding to the excitations into the S1 state plus the third and fourth triplet states in our calculations (1^3B_1 and 1^3A_2), and finally one (dotted−dashed line) where excitations

into the third, fourth, fifth, and sixth triplet states plus the first, third, and fourth singlet states in our calculations are added together (the second singlet state in our calculations appears at higher energy than our fourth, and sometimes our third, in more accurate calculations).

The size and shape of the measured and calculated excitation functions for ΔE = 3.72 and 4.61 eV agree extremely well. This agreement is similar to that obtained for pyrimidine,[33] but in that case, the quantity compared was integral excitation cross sections (obtained from the integration over all angles of the excitation functions). Here, we show the agreement to be excellent for specific angles. For ΔE = 5.41 eV, the agreement is not as good; it is clear that inclusion of three states in the calculation produces an excitation function that is much smaller than the experimental one. One needs to include at least seven states to obtain a calculated cross section of similar size to the experimental one. This does not necessarily indicate that all seven states contribute to this excitation function. The quality of description of the electronic states of thiophene in our calculations gets worse as their energy increases, in part but not only, because some of these states have Rydberg character. Therefore, the calculations will clearly provide a less accurate description of electronic excitation into higher-lying states. It is this effect that may be leading to an inaccurate excitation function for ΔE = 5.41 eV and the need to include more states than are actually contributing to the measurement.

The positions of those resonances identified in the excitation functions show good agreement with our calculated resonances. As expected, the calculated resonance positions are at higher energies than the experimental ones. There may be two reasons for this: first, the energies of the parent states are overestimated in our calculation, and second, it is expected that the polarization effects will not be fully described in a CC calculation. The latter is likely to be a smaller effect for thiophene as the shape resonances are in fairly good agreement with experiment. A similar comparison for pyrimidine[33] produced very similar agreement (including the absence of some calculated resonances in the EELS cross sections); the shifts are somewhat smaller in this case but, as for pyrimidine, increase as the resonance energy increases.

It is not surprising that some of the resonances identified in our calculations cannot be seen in the EELS experiments; not all core-excited resonances have a strong effect in the electronic excitation cross sections. Those calculated resonances that are visible appear, as expected, in the excitation function of their parent states: the 1^2A_2 one appears in the T1, the 1^2B_1 appears both in T1 and T2, the 2^2B_1 appears again in both T1 and T2, and the 2^2A_2 appears in all three. Of the resonances that are not apparent in the experimental excitation functions, only the 3^2B_1 (at around 9 eV in our calculations) has either the T1, T2, or S2 as the main parent state (specifically, the T1).

Comparison with DEA Results. The DEA experiments of Muftakhov et al. are hard to correlate with the resonances that we identified, but some links can be made. The ion yields for H-loss and the formation of a fragment with mass 32 have a peak at around 3.4−3.5 eV. The only possible resonance on our calculations that this may be linked to is the higher-lying pure shape π^* resonance located at around 2.9 eV. Alternatively, the peak in these yields could correspond to a narrow Feshbach resonance that we have failed to identify whose parent is the lowest excited state (the 1^3B_2). The ion yields for several fragments (among them the one coming from single H-loss) display peaks at around 5.3, 5.5, and 5.8 eV. Again, the only resonance that we describe in our calculations that could be linked to these peaks is the 1^2A_2 at ∼5.7 eV seen by the EELS closer to 5.4−5.5 eV. Peaks in the mass spectra in the range of 6.15−6.4 eV could be linked to the 1^2B_1 resonance that we observe at 6.7 eV and the EELS at 6.4−6.45 eV (the 1^2B_2 resonance at around 6.9 eV is much shorter lived and less likely to lead to dissociation). Finally, several peaks in the 8.5−8.9 eV range could be linked to one or several of the resonances that we describe in the 8.98−9.45 eV range. Muftakhov et al. do not report peaks in the mass spectra below 3.3 eV.

CONCLUSIONS

We have performed R-matrix calculations and EELS experiments for electron scattering from thiophene in order to identify and characterize its core-excited resonances. Comparison of measured and calculated excitation functions for two different angles and three different energy losses show very good agreement; both their size and shape agree very well, at least for the two energy losses where it is clear which states are being excited. This indicates that the calculations are modeling the physics of the collision accurately, despite the fact that our usual strategy for determining how to model the polarization effects (i.e., how many virtual orbitals are required for their description) does not seem to work particularly well for this system. It also demonstrates that it is now possible to provide quantitatively accurate cross sections for low-energy electronic excitation of low-lying states of biologically relevant molecules.

Our calculated results for the pure shape resonances agree well with previous calculations and experiments, although some uncertainty persists as to the accurate position of the rather wide σ^* resonance. Four core-excited or mixed core-excited resonances described by our calculations are visible in the excitation functions, although, as expected, the calculated ones appear higher in energy. These are, on the whole, the longer-lived (i.e., narrower) resonances identified. A feature appears at around 4.2 eV in the excitation function that we believe may correspond to a poorly described (in the calculations) pure shape A_1 resonance. Another six resonances are identified in our calculations. Finally, some of the core-excited resonances can be linked to the DEA spectra of Muftakhov et al.[12]

ASSOCIATED CONTENT

Supporting Information

The Supporting Information is available free of charge on the ACS Publications website at DOI: 10.1021/acs.jpca.7b11865.

Energy loss spectra measured in the forward and backward directions in order to identify the excited states of thiophene and experimental elastic differential cross sections (PDF)

AUTHOR INFORMATION

Corresponding Author

*E-mail: jimena.gorfinkiel@open.ac.uk.

ORCID

Jimena D. Gorfinkiel: 0000-0001-9264-3932

Present Address

§K.R.: Laboratório de Colisões Atómicas e Moleculares, CEFITEC, Departamento de Física, Faculdade de Ciências e Tecnologia, Universidade Nova de Lisboa, Campus de Caparica, Lisboa, 2829-516 Portugal.

Notes

The authors declare no competing financial interest.

■ ACKNOWLEDGMENTS

This work used the ARCHER UK National Supercomputing Service (http://www.archer.ac.uk). M.A. and K.R. acknowledge support by Project No. 200020-144367/1 of the Swiss National Science Foundation. A.L. was supported by Fundação para a Ciência e a Tecnologia (FCT-MCTES), Radiation Biology and Biophysics Doctoral Training Programme (RaBBiT, PD/00193/2012); UID/Multi/04378/2013 (UCIBIO); UID/FIS/00068/2013 (CEFITEC). K.R. acknowledges the Swiss National Science Foundation for an EPM fellowship.

■ REFERENCES

(1) Boudaïffa, B.; Cloutier, P.; Hunting, D.; Huels, M. A.; Sanche, L. Resonant Formation of DNA Strand Breaks by Low-energy (3 to 20 eV) Electrons. *Science* **2000**, *287*, 1658−1660.

(2) Fabrikant, I. I.; Eden, S.; Mason, N. J.; Fedor, J. In *Advances in atomic, molecular, and optical physics*; Ennio Arimondo, C. C. L., Yelin, S. F., Eds.; Academic Press, 2017; Vol. *66*; pp 545−657.

(3) Alizadeh, E.; Sanche, L. Precursors of Solvated Electrons in Radiobiological Physics and Chemistry. *Chem. Rev.* **2012**, *112*, 5578−5602.

(4) Baccarelli, I.; Bald, I.; Gianturco, F. A.; Illenberger, E.; Kopyra, J. Electron-induced Damage of DNA and its Components: Experiments and Theoretical Models. *Phys. Rep.* **2011**, *508*, 1−44.

(5) Gorfinkiel, J. D.; Ptasińska, S. Electron Scattering from Molecules and Molecular Aggregates of Biological Relevance. *J. Phys. B: At., Mol. Opt. Phys.* **2017**, *50*, 182001.

(6) Gramec, D.; Peterlin, L.; Sollner, M. Bioactivation Potential of Thiophene-containing Drugs. *Chem. Res. Toxicol.* **2014**, *27*, 1344−1358.

(7) Hedhili, M. N.; Cloutier, P.; Bass, A. D.; Madey, T. E.; Sanche, L. Electron Stimulated Desorption of Anionic Fragments from Films of Pure and Electron-irradiated Thiophene. *J. Chem. Phys.* **2006**, *125*, 094704.

(8) Staykov, A.; Areephong, J.; Browne, W. R.; Feringa, B. L.; Yoshizawa, K. Electrochemical and Photochemical Cyclization and Cycloreversion of Diarylethenes and Diarylethene-capped Sexithiophene Wires. *ACS Nano* **2011**, *5*, 1165−1178.

(9) Dimitrakopoulos, C.; Malenfant, P. Organic Thin Film Transistors for Large Area Electronics. *Adv. Mater.* **2002**, *14*, 99−117.

(10) Liang, Y.; Yu, L. Development of Semiconducting Polymers for Solar Energy Harvesting. *Polym. Rev.* **2010**, *50*, 454−473.

(11) Murphy, A.; Frechet, J. Organic Semiconducting Oligomers for Use in Thin Film Transistors. *Chem. Rev.* **2007**, *107*, 1066−1096.

(12) Muftakhov, M. V.; Asfandiarov, N.; Khvostenko, V. I. Resonant Dissociative Electron Attachment of Electrons to Molecules of Five-membered Heterocyclic Compounds and Lactams. *J. Electron Spectrosc. Relat. Phenom.* **1994**, *69*, 165−175.

(13) Asmis, K. R. Ph.D. thesis, Université de Fribourg, Switzerland, 1996.

(14) Modelli, A.; Burrow, P. Electron Attachment to the Aza-derivatives of Furan, Pyrrole and Thiophene. *J. Phys. Chem. A* **2004**, *108*, 5721−5726.

(15) da Costa, R.; do N. Varella, M.; Lima, M.; Bettega, M. Low-energy Electron Collisions with Thiophene. *J. Chem. Phys.* **2013**, *138*, 194306.

(16) Vinodkumar, M.; Desai, H.; Vinodkumar, P. Electron Induced Chemistry of Thiophene. *RSC Adv.* **2015**, *5*, 24564−24574.

(17) Mozejko, P.; Ptasinska-Denga, E.; Szmytkowski, C. Cross Sections for Electron Collision with Five-membered Ring Heterocycles. *Eur. Phys. J. D* **2012**, *66*, 20659−20666.

(18) Tennyson, J. Electron-molecule Collision Calculations Using the R-matrix Method. *Phys. Rep.* **2010**, *491*, 29−76.

(19) Carr, J. M.; Galiatsatos, P. G.; Gorfinkiel, J. D.; Harvey, A. G.; Lysaght, M. A.; Madden, D.; Mašín, Z.; Plummer, M.; Tennyson, J.; Varambhia, H. N. UKRmol: a Low-energy Electron- and Positron-molecule Scattering Suite. *Eur. Phys. J. D* **2012**, *66*, 20653−20656.

(20) Burke, P. G. *R-matrix Theory of Atomic Collisions: Application to Atomic, Molecular and Optical Processes*; Springer, 2011.

(21) Fabrikant, I. I. Long-range Effects in Electron Scattering by Polar Molecules. *J. Phys. B: At., Mol. Opt. Phys.* **2016**, *49*, 222005.

(22) Mašín, Z.; Gorfinkiel, J. D.; Jones, D. B.; Bellm, S. M.; Brunger, M. J. Elastic and Inelastic Cross Sections for Low-energy Electron Collisions with Pyrimidine. *J. Chem. Phys.* **2012**, *136*, 144310−144320.

(23) Norcross, D. W.; Padial, N. T. The Multipole-extracted Adiabatic-nuclei Approximation for Electron-molecule Collisions. *Phys. Rev. A: At., Mol., Opt. Phys.* **1982**, *25*, 226−238.

(24) Tashiro, M.; Morokuma, K.; Tennyson, J. *R*−matrix Calculation of Differential Cross Sections for Low-energy Electron Collisions with Ground-state and Electronically Excited-state O_2 Molecules. *Phys. Rev. A: At., Mol., Opt. Phys.* **2006**, *74*, 022706−022714.

(25) Hazi, A. U. Behavior of the Eigenphase Sum Near a Resonance. *Phys. Rev. A: At., Mol., Opt. Phys.* **1979**, *19*, 920−922.

(26) Mašín, Z.; Gorfinkiel, J. D. Shape and Core Excited Resonances in Electron Collisions with Diazines. *J. Chem. Phys.* **2012**, *137*, 204312.

(27) Shimamura, I.; Cleanthes, E.; Nicolaides, A.; Sabin, J. *Advances in Quantum Chemistry*; Academic, 2012.

(28) Smith, F. T. Lifetime Matrix in Collision Theory. *Phys. Rev.* **1960**, *118*, 349−356.

(29) Allan, M.; Winstead, C.; McKoy, V. Electron Scattering in Ethene: Excitation of the $\tilde{a}\ ^3B_{1u}$ State, Elastic Scattering and Vibrational Excitation. *Phys. Rev. A: At., Mol., Opt. Phys.* **2008**, *77*, 042715.

(30) Allan, M. Electron Collisions with CO: Elastic and Vibrational Excitation Cross Sections. *Phys. Rev. A: At., Mol., Opt. Phys.* **2010**, *81*, 042706.

(31) Regeta, K.; Allan, M. Absolute Cross Sections for Electronic Excitation of Furan by Electron Impact. *Phys. Rev. A: At., Mol., Opt. Phys.* **2015**, *91*, 012707.

(32) Regeta, K.; Allan, M.; Winstead, C.; McKoy, V.; Mašín, Z.; Gorfinkiel, J. D. Resonance Effects in Elastic Cross Sections for Electron Scattering on Pyrimidine: Experiment and Theory. *J. Chem. Phys.* **2016**, *144*, 024301.

(33) Regeta, K.; Allan, M.; Mašín, Z.; Gorfinkiel, J. D. Absolute Cross Sections for Electronic Excitation of Pyrimidine by Electron Impact. *J. Chem. Phys.* **2016**, *144*, 024302.

(34) Gopalan, A.; Bömmels, J.; Götte, S.; Landwehr, A.; Franz, K.; Ruf, M. W.; Hotop, H.; Bartschat, K. A Novel Electron Scattering Apparatus Combining a Laser Photoelectron Source and a Triply Differentially Pumped Supersonic Beam Target: Characterization and Results for the $He^-(1s2s^2)$ Resonance. *Eur. Phys. J. D* **2003**, *22*, 17−29.

(35) Allan, M. Measurement of the Elastic and $v = 0 \rightarrow 1$ Differential Electron-N_2 Cross Sections Over a Wide Angular Range. *J. Phys. B: At., Mol. Opt. Phys.* **2005**, *38*, 3655−3672.

(36) Nickel, J. C.; Zetner, P. W.; Shen, G.; Trajmar, S. Principles and Procedures for Determining Absolute Differential Electron-molecule (Atom) Scattering Cross Sections. *J. Phys. E: Sci. Instrum.* **1989**, *22*, 730−738.

(37) Nesbet, R. K. Variational Calculations of Accurate e^- − He Cross Sections Below 19 eV. *Phys. Rev. A: At., Mol., Opt. Phys.* **1979**, *20*, 58−70.

(38) McClellan, A. *Tables of experimental dipole moments*; W.H. Freeman, 1963.

(39) Gussoni, M.; Rui, R.; Zerbi, G. Electronic and Relaxation Contribution to Linear Molecular Polarizability. An Analysis of the Experimental Values. *J. Mol. Struct.* **1998**, *447*, 163−215.

(40) *NIST Standard reference database*. http://http://cccbdb.nist.gov (accessed Oct. 4, 2017).

(41) Palmer, M. H.; Walker, I. C.; Guest, M. F. The Electronic States of Thiophene Studied by Optical (VUV) Absorption, Near-threshold Electron Energy Loss (EEL) Spectroscopy and Ab Initio Multi-Reference Configuration Interaction Calculations. *Chem. Phys.* **1999**, *241*, 275−296.

(42) Haberkern, H.; Asmis, K.; Allan, M.; Swiderek, P. Triplet States in Oligomeric Materials: Electron Energy Loss Spectroscopy of Thiophene and Bithiophene and Extrapolation to the Polymer. *Phys. Chem. Chem. Phys.* **2003**, *5*, 827−833.

(43) Flicker, W.; Mosher, O.; Kuppermann, A. Electron Impact Investigation of Electronic Excitations in Furan, Thiophene, and Pyrrole. *J. Chem. Phys.* **1976**, *64*, 1315−1321.

(44) Salzmann, S.; Kleinschmidt, M.; Weinkkauf, J. T. R.; Marian, C. M.; et al. Excited States of Thiophene: Ring Opening as Deactivation Mechanism. *Phys. Chem. Chem. Phys.* **2008**, *10*, 380−392.
(45) Weinkauf, R.; Lehr, L.; Schlag, E. W.; Salzmann, S.; Marian, C. M. Ultrafast Dynamics in Thiophene Investigated by Femtosecond Pump Probe Photoelectron Spectroscopy and Theory. *Phys. Chem. Chem. Phys.* **2008**, *10*, 393−404.
(46) Holland, D. M. P.; Trofimov, A. B.; Seddon, E. A.; Gromov, E. V.; Korona, T.; de Oliveira, N.; Archer, L. E.; Joyeux, D.; Nahon, L. Excited Electronic States of Thiophene: High Resolution Photoabsorption Fourier Transform Spectroscopy and Ab Initio Calculations. *Phys. Chem. Chem. Phys.* **2014**, *16*, 21629−21644.
(47) Wan, J.; Hada, M.; Ehara, M.; Nakatsuji, H. Electronic Excitation Spectrum of Thiophene Studied by Symmetry-adapted Cluster Configuration Interaction Method. *J. Chem. Phys.* **2001**, *114*, 842.
(48) Serrano-Andrés, L.; Merchán, M.; Fulscher, M.; Roos, B. O. A Theoretical Study of the Electronic Spectrum of Thiophene. *Chem. Phys. Lett.* **1993**, *211*, 125−134.
(49) Kleinschmidt, M.; Tatchen, J.; Marian, C. Spin-orbit Coupling of DFT/MRCI Wavefunctions: Method, Test Calculations, and Application to Thiophene. *J. Comput. Chem.* **2002**, *23*, 824−833.
(50) Werner, H.-J.; Knowles, P. J.; Knizia, G.; Manby, F. R.; Schütz, M.; Celani, P.; Györffy, W.; Kats, D.; Korona, T.; Lindh, R.; et al. *MOLPRO*, version 2015.1, a package of ab initio programs. http://www.molpro.net (2015).
(51) Jones, E.; Moodie, I. M. The Synthesis and Absorption Spectra of the Isomeric Dithienyl Sulphides. *Tetrahedron* **1965**, *21*, 2413−2420.
(52) Di Lonardo, G.; Galloni, G.; Trombetti, A.; Zauli, C. Electronic Spectrum of Thiophen and Some Deuterated Thiophens. *J. Chem. Soc., Faraday Trans. 2* **1972**, *68*, 2009−2016.
(53) Van Veen, E. H. Triplet $\pi-\pi^*$ Transitions in Thiophene, Furan and Pyrrole by Low-energy Electron Impact Spectroscopy. *Chem. Phys. Lett.* **1976**, *41*, 535−539.
(54) Nyulászi, L.; Veszprémi, T. Near Ultraviolet Spectrum of Thiophene and its Derivatives. *Chem. Scr.* **1986**, *26*, 629−634.
(55) Hakansoon, R.; Nordén, B.; Thulstrup, E. Magnetic Circular Dichroism of Heterocycles: Thiophene. *Chem. Phys. Lett.* **1977**, *50*, 306−308.
(56) Loupas, A.; Gorfinkiel, J. D. Resonances in Low-energy Electron Scattering from para-Benzoquinone. *Phys. Chem. Chem. Phys.* **2017**, *19*, 18252−18261.